Immunity, Vol. 17, 83–94, July, 2002, Copyright ©2002 by Cell Press

Structural Snapshot of Aberrant Antigen Presentation Linked to Autoimmunity: The Immunodominant Epitope of MBP Complexed with I-A^u

Xiao-lin He,[1] Caius Radu,[2] John Sidney,[3] Alessandro Sette,[3] E. Sally Ward,[2] and K. Christopher Garcia[1,4]

[1]Department of Microbiology and Immunology
Stanford University School of Medicine
Stanford, California 94305

[2]Center for Immunology and
Cancer Immunobiology Center
University of Texas-Southwestern Medical Center
Dallas, Texas 75390

[3]Epimmune Inc.
San Diego, California 92121

Summary

Murine experimental allergic encephalomyelitis (EAE) is a useful model for the demyelinating, autoimmune disease multiple sclerosis. In the EAE system, the immunodominant N-terminal epitope of myelin basic protein (MBP) is an unusually short, weakly binding peptide antigen which elicits highly biased TCR chain usage. In the 2.2 Å crystal structure of I-A^u/MBP1-11 complex, only MBP residues 1–7 are bound toward one end of the peptide binding cleft. The fourth residue of MBP1-11 is located in an incompatible p6 pocket of I-A^u, thus explaining the short half-life of I-A^u complexed with Ac1-11. MBP peptides extended at the C terminus of Ac1-11 result in dramatic affinity increases, likely attributed to register shifting to a higher affinity cryptic epitope, which could potentially mask the presentation of the immunodominant MBP1-11 peptide during thymic education.

Introduction

The activation of CD4$^+$ T cells by peptide-MHC complexes is a key event in the induction of autoimmune diseases such as multiple sclerosis (MS) and rheumatoid arthritis (RA). For MS, murine experimental allergic encephalomyelitis (EAE) represents an intensively studied model system for understanding autoimmunity to neural self-antigens such as myelin basic protein (MBP), myelin oligodendrocyte protein (MOG), and proteolipid protein (PLP) (Goverman, 1999; Steinman, 1996; Zamvil and Steinman, 1990).

Class II MHC I-A molecules are usually the restriction elements for murine autoimmune models (Tisch and McDevitt, 1996). Structural features of I-A^d, I-A^k, and I-A^{g7} are consistent with promiscuous peptide binding motifs in I-A epitopes (Corper et al., 2000; Fremont et al., 1998; Latek et al., 2000; Scott et al., 1998), in contrast to the more restricted motifs found in I-E (Rammensee et al., 1995). The somewhat promiscuous nature of I-A may give rise to inefficient negative selection of autoreactive T cells. Currently, a clear structural relationship between an autoimmune MHC-peptide complex and disease has not been demonstrated (Corper et al., 2000; Latek et al., 2000; Lee et al., 2001; Smith et al., 1998). In the case of I-A^{g7} from the nonobese diabetic mouse (NOD), a widening of the p9 MHC pocket was observed, but the link to disease is not obvious (Corper et al., 2000; Latek et al., 2000).

The immunodominant encephalitogenic T cell epitope of MBP, in mice of the H-2^u haplotype (PL/J or B10.PL), is the acetylated N-terminal 9- or 11-mer (Ac1-11, *Ac*ASQYRPSQRHG). The Ac1-11 epitope in the context of I-A^u has been extensively characterized in functional studies, which have revealed a number of unusual features in this system (Acha-Orbea et al., 1988; Urban et al., 1988; Fairchild et al., 1993; Fugger et al., 1996; Gautam et al., 1992a, 1992b; Mason et al., 1995; Wraith et al., 1989, 1992; Pearson et al., 1999). First, a posttranslational modification to the MBP peptide, N-terminal acetylation, is required for induction of EAE (Zamvil et al., 1986). Second, despite being the immunodominant epitope in vivo, Ac1-11 binds to I-A^u very weakly ($t_{1/2} < 15$ min) (Fairchild et al., 1993; Fugger et al., 1996; Mason et al., 1995). This low affinity results in escape of I-A^u/Ac1-11-specific T cells from central tolerance induction, resulting in immunodominance of this epitope following immunization of mice with MBP. Consistent with this, in MBP-deficient mice other epitopes of MBP become immunodominant (Harrington et al., 1998). Substitution of position four lysine (MBP4-Lys) of MBP with several other residues (e.g., Ala, Tyr) greatly increases the stability of the I-A^u-peptide complexes. Surprisingly, an inverse correlation has been observed between the affinity of P4 variants of Ac1-9 for I-A^u and the ability of the peptide to induce EAE (Anderton et al., 2001; Fairchild et al., 1993; Mason et al., 1995; Wraith et al., 1989).

A still further unusual feature is that I-A^u/Ac1-11-specific T cells, the vast majority of which exhibit a highly biased TCR chain usage for Vβ8.2, can respond to truncated MBP peptides as short as Ac1-6 (Gautam et al., 1994). Most peptide antigens restricted to class II MHC are between 12–15 amino acids in length and traverse the length of the MHC groove. Hence, it has been speculated from modeling studies that only the N-terminal six amino acids of Ac1-11 lie in the MHC binding groove (Gautam et al., 1994; Lee et al., 1998). This would result in a partially empty MHC groove, presenting a truncated peptide to a TCR, which would be unprecedented.

Finally, it has been shown that cryptic epitopes (Sercarz et al., 1993) within the MBP sequence could, in principle, compete with the immunodominant Ac-11 epitope for binding to I-A^u (Fairchild et al., 1996). Whether such cryptic epitopes are generated during natural peptide processing in the class II MHC peptide loading pathway is still uncertain. However, such epitopes, if generated from naturally processed MBP, would be expected to effect the development of the T cell repertoire in H-2^u mice.

Here we present a structural analysis of a recombinant I-A^u/MBP1-11 complex in tandem with MBP peptide substitution studies. Strikingly, we find that the I-A^u peptide binding groove contains only the first seven resi-

[4]Correspondence: kcgarcia@stanford.edu

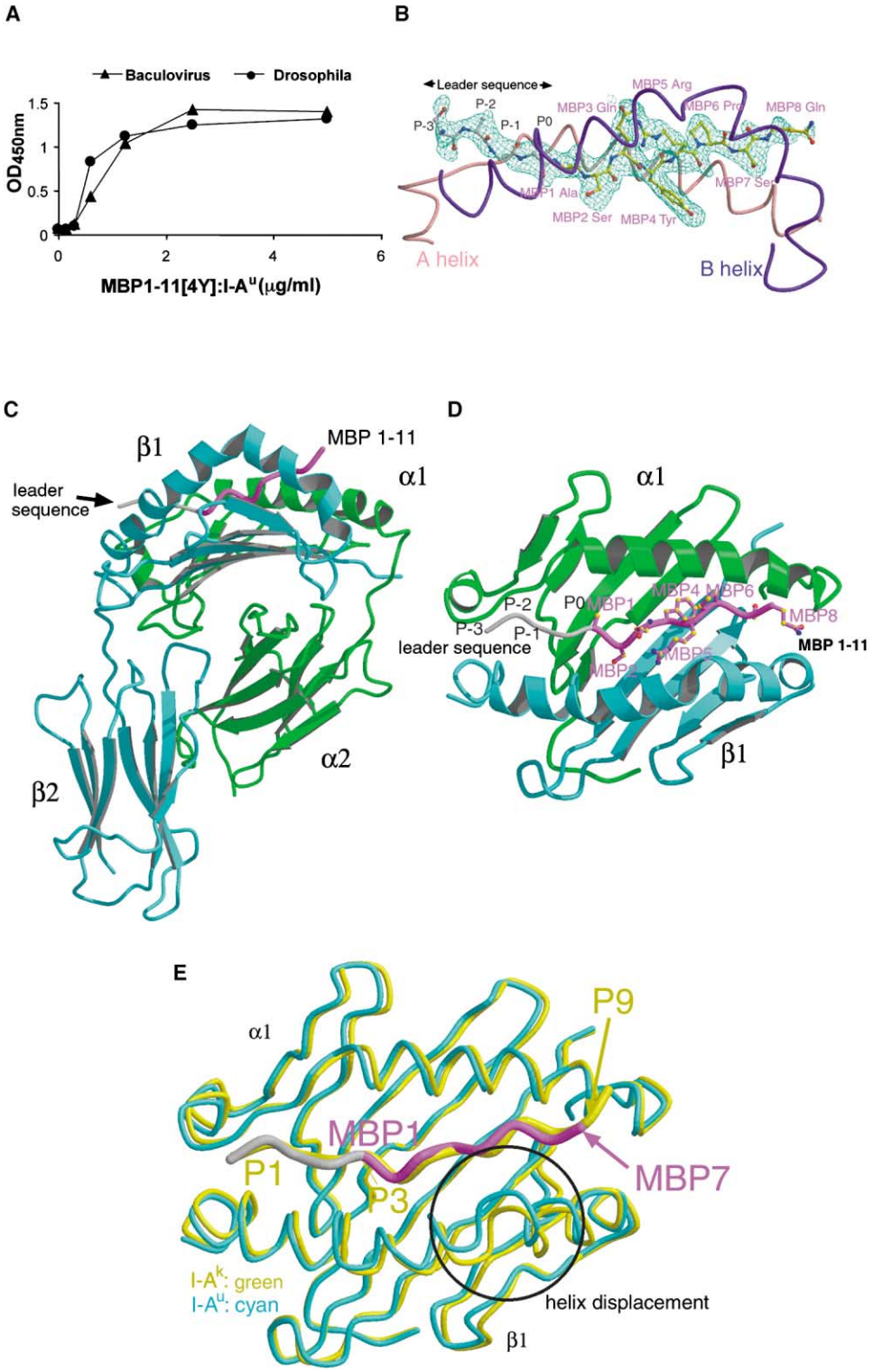

Figure 1. Bioactivity and Three-Dimensional Structure of I-A^u/MBP1-11

(A) Engineered, recombinant I-A^u/MBP1-11(P4-Tyr), expressed from *Drosophila melanogaster* (crystallized for this study) and baculovirus (Radu et al., 1998), effectively stimulate the Ac1-11-specific T cell hybridoma 172.10 (Urban et al., 1988) (see Experimental Procedures for details).

(B) Side view of the electron density of the MBP peptide, including the residual leader peptide after processing. The electron density is a 2.2 Å SIGMAA omit map of the peptide (Read, 1986). In front of the electron density is a tube representation of the β chain helix, and in back of the peptide is the α chain helix.

(C and D) Side view (C) and top view (D) (into the peptide binding groove) of ribbons representation of the I-A^u/MBP1-11 structure. α chain

dues of the MBP1-11 peptide. With the exception of the hydrophobic p6 pocket, the molecular nature of the I-A^u peptide binding groove is largely devoid of highly specific peptide recognition features. Extensions to the Ac1-11 C terminus dramatically enhance the affinity for I-A^u, a phenomenon which appears to be due to register shifting to a cryptic epitope proximal to the immunodominant sequence.

Results

Expression of I-A^u/MBP1-11

Due to the short half-life of I-A^u complexed with native MBP Ac1-11 (Fairchild et al., 1993; Mason et al., 1995; Fugger et al., 1996) and the necessity of a posttranslational acetylation of the peptide N terminus, expression of recombinant complexes required the design of biochemically stable protein, which behaved in all ways like the native molecule (Figure 1A). I-A^u was expressed from *Drosophila melanogaster* with the MBP1-11 peptide covalently linked to the N terminus of the I-A^u β chain through an eight-residue linker. Earlier studies indicated that empty I-A^u or I-A^u complexed with the wild-type MBP1-11 is unstable (Radu et al., 2000), most likely because of the low affinity of this epitope for I-A^u. We therefore used the higher affinity MBP4-Tyr mutant, which allowed secretion of the stable complex. This substitution enhances binding of the peptide to I-A^u by 1500-fold (Fugger et al., 1996), without affecting T cell recognition (Figure 1A) (Anderton et al., 2001; Wraith et al., 1992).

N-Terminal Residues of Peptide in the Groove

To recapitulate the posttranslational acetylation of the MBP N terminus, we engineered a glycine residue at MBP-0, whose carbonyl group and α-carbon atom faithfully mimic the acetyl group found in MBP. N-terminal sequencing of the secreted proteins revealed that three additional residues from the leader sequence (Ser-Arg-Gly at P-3, P-2, and P-1, respectively) remain at the amino-terminus after processing (Figure 1B). The leader sequence-derived P0-Gly and P-1-Gly main chain N atoms form H bonds to I-A^u groove residues in a fashion similar to that seen in longer class II binding peptides, having the resultant effect of ordering the artificial leader extension as it extends out of the groove (Figures 1B and 1D). The additional leader peptide residues do not influence the functional properties of the I-A^u/MBP complex relative to the natural I-A^u complexed with free peptide (Figure 1A). Recombinant I-A^u/MBP1-11 complexes were secreted from both *Drosophila melanogaster* and baculovirus using different signal sequences (with different processing sites), and both complexes are effective in stimulating IL-2 secretion by I-A^u-Ac1-11-specific T cell hybridomas/transfectants (Figure 1A) and interacting with recombinant Ac1-11-specific TCRs. The structure was determined to 2.2 Å (Table 1).

Table 1. Crystallographic Statistics

Data Collection	
Space group	$C222_1$
Unit cell (Å) (a, b, c)	99.15, 110.59, 94.84
Source	SSRL, BL7-1
Resolution (Å) (highest resolution shell)	50.0–2.2 (2.3–2.2)
Measured reflections	144,694
Unique reflections	26,280
Completeness (%)	98.3 (98.5)
I/σ (I)	6.7 (1.6)
R_{merge} (%)[a]	8.0 (45.0)
Refinement Statistics	
Resolution range (Å)	50.0–2.3 (2.3–2.2)
R_{cryst}[b]	0.248 (0.323)
R_{free}[c]	0.276 (0.354)
No. of atoms (protein solvent)	3157, 450
Average B factors (Å^2) (I-A^u, MBP1-11, oligosaccharides, solvents)	49.5, 57.4, 86.3, 56.8
Rms deviation from ideality	
Bond lengths (Å)	0.008
Bond angles (°)	1.4
Dihedrals (°), impropers (°)	25.5, 0.8
Bonded B factors (Å^2) main chain, side chain	2.2, 2.9
Ramachandran plot (%) (favored, allowed, generous, disallowed)	87.3, 12.4, 0.3, 0

[a] $R_{merge} = \Sigma_{hkl}|I - <I>|/\Sigma_{hkl}I$, where I is the intensity of unique reflection hkl, and $<I>$ is the average over symmetry-related observation of unique reflection hkl.
[b] $R_{cryst} = \Sigma||F_{bobs} - F_{calc}|/\Sigma F_{obs}$, where F_{obs} and F_{calc} are the observed and the calculated structure factors, respectively.
[c] R_{free} is R using 5% of reflections sequestered before refinement.

Overview of the Structure

The polypeptide main chain of the I-A^u $\alpha\beta$ heterodimer is representative of the overall fold of other MHC II and I-A molecules previously reported (Figure 1C) (Corper et al., 2000; Fremont et al., 1998; Latek et al., 2000; Scott et al., 1998; Stern and Wiley, 1994). The amino-terminal domains of the heterodimer together form a characteristic peptide binding groove like other class II molecules (Figure 1D). The I-A^u backbone residues superimpose closely with I-A^k, I-A^d, and I-A^{g7} giving low root mean square deviations of 0.57, 0.59, and 0.60 Å for all common Cα positions, respectively (Figure 1E). One noticeable exception involves a displacement of one turn of the I-A^u α helix, in the 60-71β region toward the peptide, which results in a narrowing at the end of the peptide binding groove (Figure 1E) (discussed below).

The MBP1-11 Peptide Partially Occupies the Groove

The most striking feature of this structure is that the I-A^u peptide binding groove contains only the first seven

is green, β chain is light blue, the peptide is colored purple, and the residual leader peptide remaining from the expression vector is in gray. (E) The backbones of I-A^u and I-A^k (Fremont et al., 1998) were superimposed in this view into the peptide binding groove. I-A^u is colored cyan, with the MBP peptide purple and leader peptide gray, and I-A^k is colored green, with the HEL peptide yellow. The location of the β chain helix displacement toward the MBP peptide is circled.

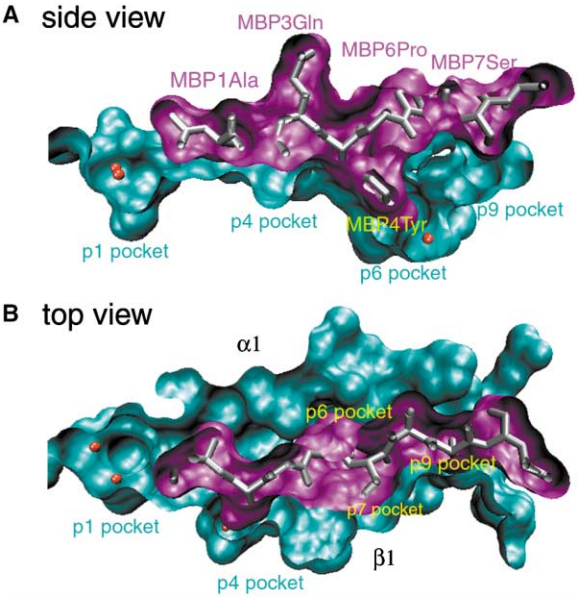

Figure 2. Molecular Surface Complementarity between the I-A^u Groove and the MBP Peptide

To depict the natural Ac-11 peptide, the residual leader peptide residues have been removed from the structure. Molecular surfaces of I-A^u (blue) with bound MBP peptide (purple) were produced, and the figures show planar cross sections through these surfaces to illustrate the shape and complementarity between peptide and MHC, as well as unfilled pockets and ordered water molecules (red spheres). The MBP peptide is shown within the surface as silver sticks. (A) is a side view, as in Figure 1C, and (B) is the groove viewed from the top, as in Figure 1D. Due to the planar cross section of the convoluted surfaces, some residues of the peptide are sliced out of view, such as P5-Arg, which extends toward the reader in (A) and (B). In (A), the large and spacious p6 pocket is apparent, as are the ordered water molecules in the p1 and p6 pockets. In (B), the empty p1 pocket is in the far left of the blue I-A^u molecular surface, and the p7 pocket, where the P5-Arg resides, extends sideways but does not appear occupied by P5-Arg due to the cross section. The molecular surfaces were produced using a 1.4 Å probe radius.

residues of the MBP1-11 peptide (Figures 1 and 2), indicating that the natural Ac1-11 complex leaves the p1 and p2 pockets empty, as depicted in Figure 2. Previous crystal structures of class II MHC-peptide complexes contain grooves completely filled with 12–17 amino acid peptides that freely protrude from the ends of the open groove (e.g., I-A^k in Figure 1E). The MBP1-11 peptide is bound to I-A^u in an extended type II poly-proline conformation, as previously observed in other class II structures, except that the register of peptide is shifted by two residues such that the MBP1-Ala resides where the P3 peptide residue is normally located in canonically registered class II peptide-MHC complexes (Figure 1E). As discussed, three additional N-terminal residues from the linker sequence remain connected to the amino terminus of the peptide (Figure 1), but the p1 pocket is not occupied by a peptide side chain since P-1 is a glycine. The absence of side chains in the p1 and p2 pockets presumably resembles the empty pockets which would be found in vitro and in vivo for I-A^u complexed to naturally processed Ac1-11 (Figure 2). At the C-terminal end of the covalent peptide, MBP residues eight, nine, ten, and eleven, plus the eight residue Gly-Ser linker connected to the β chain N terminus, lie outside of the groove and have disordered electron density (Figure 1B). The recombinant, covalent peptide complexes potently activate Ac1-11-specific T cells (Figure 1B). Therefore, the register of the natural Ac1-11 peptide is the same as the covalently bound peptide in this structure, which is also consistent with functional and modeling studies of Ac1-11 bound to I-A^u (Lee et al., 1998).

The unique binding mode of the MBP1-11 peptide to I-A^u is determined by the occupied MHC anchor positions at p4, p6, and p9 (Table 2); these residues would normally comprise TCR-contact residues. As a result, the exposed regions (MBP3-Gln, MBP6-Pro) of the peptide, which would point downward and fill MHC pockets in a canonical register, now point outward and comprise the TCR-contact residues (Figure 3).

Implications for Empty MHC

The p1 pocket of I-A^u is occupied by several ordered water molecules, which probably contribute to the structural integrity of the pocket (Figure 2). The structure of this pocket in I-A^u is not perturbed in comparison with MHC structures whose p1 pocket is filled with an amino acid side chain, suggesting that incomplete occupancy is sufficient to stabilize the MHC groove, which has been shown to exist as a molten globule, or partially folded protein, in a completely empty state (Bouvier and Wiley, 1998; Zarutskie et al., 1999). The I-A^d/OVA and HA structures show a poor peptide fit in the p1 pocket due to the use of undersized side chains at the P1 peptide residue (Scott et al., 1998). This common theme in I-A structures implies that p1 pocket usage is not crucial for peptide binding to I-A molecules, which may contribute to their promiscuity (Scott et al., 1998).

N-Terminal Acetylation of the MBP Peptide Is Required for MHC Binding

As MBP is naturally acetylated at its N terminus, Ac1-11 is a rare case of a peptide antigen which requires a posttranslational modification for MHC presentation (the other example being the formylated peptide bound to H2M3 [Wang et al., 1995]). The nonacetylated MBP1-11 peptide is incapable of inducing EAE (Zamvil et al., 1986). In the recombinant protein, the peptide bond of the artificially engineered P0-Gly mimics the acetyl group (Figures 1C and 3A). Structurally, the carbonyl of the P0-Gly is hydrogen bonded to the Nδ2 of Asn82β in an H-bonding interaction similar to that seen in a normal length peptide main chain carbonyl (Figure 3A and Table 2). The hydrogen-bonded acetyl group not only enhances the peptide binding affinity but also neutralizes the N terminus, which would otherwise be charged and energetically unfavorable for burial within the groove. As opposed to the buried terminal peptide charges in class I MHC (Madden, 1995), no other MHC II/peptide complexes have their charged N or C termini within the groove (Stern and Wiley, 1994); rather, they extend out of the open ends of the groove (e.g., I-A^k in Figures 1E and 4). In MBP1-11, the neutralized P1 N-terminal nitrogen atom resides within a solvent exposed, hydrophobic patch composed of Phe54α, Phe24α, and

Table 2. Intermolecular Contacts between I-A^u and MBP1-11 Peptide

Hydrogen Bonds between MBP1-11 Peptide and I-A^u		
MBP 1-11	**I-A^u**	**Distance (Å)**
(leader) Gly-1 N	S53α O	2.8
Gly0 N	N82β Oδ1	3.0
Gly0 O	N82β Nδ2	3.1
Ser2 N	Y9α O	3.0
Ser2 Oγ	Y26β OH	3.2
Gln3 N	E74β Oϵ2	3.2
Tyr4 N	N62α Oδ1	2.7
Arg5 N	Y30β OH	3.0
Arg5 Nη2	E74β Oϵ1	2.7
Arg5 O	Y61β OH	2.5
Pro6 O	Y66β OH	2.5
Ser7 N	N69α Oδ1	3.2
Ser7 Oγ	N69α Oδ1	3.2

Van der Waals Contacts ($<$4.5 Å cutoff)	
MBP 1-11	**Neighboring I-A^u Residues**
(leader) Ser-3	R52α, S53α, Y81β, E85β
(leader) Arg-2	S53α, Y81β
(leader) Gly-1	S53α, N82β, T86β
Gly0	Y9α, F24α, V78β, T86β
Ala1	Y9α, Y22α, F24α, F54α, V78β
Ser2	Y9α, Y26β, P13β, F11β, E74β, V78β
Gln3	F11β, E74β
Tyr4	V11α, N62α, T65α, G66α, N69α, V9β, Q10β, F11β, Y30β
Arg5	T65α, N69α, Y30β, Y61β, Y67β, R70β, E74β
Pro6	T65α, H68α, N69α, Y60β, Y61β, Y67β
Ser7	H68α, N69α, V72α, D57β, Y60β, Y61β
Gln8	P56β, Y60β

Val28β, which is a region of TCR contact in class II MHC/TCR complexes (Reinherz et al., 1999).

A Narrow p4 Pocket

The I-A^u p4 pocket is unique when compared with other mouse MHC II alleles (Figures 2 and 3). In I-A^u, the volume of the p4 pocket is substantially reduced by substitution of a Tyr residue (Tyr26β) for the more common, and substantially smaller, Leu26β found on the side wall of the pocket in other I-A alleles. The MBP2-Ser only partially occupies the p4 pocket, hydrogen bonding to Tyr26β, with the remaining space in the pocket filled by a well-ordered water molecule at the base of the cavity. The primary stabilizing force in this pocket is likely hydrophobic complementarity, as substitution of MBP2-Ser with Ala does not result in weaker binding of MBP1-11 (Figure 4) (Gautam et al., 1994).

A Cavernous p6 Pocket

Biochemical and functional studies have converged on the I-A^u p6 pocket and MBP4 residue as central to the stability of the I-A^u/MBP complex (Fairchild et al., 1993; Fugger et al., 1996; Mason et al., 1995, Pearson et al., 1999), as well as key to its interesting autoimmune characteristics in vitro and in vivo (Anderton et al., 2001; Pearson et al., 1997; Wraith et al., 1989). The p6 pocket is exceptionally large (Figures 2 and 3B) in I-A^u. This is due to smaller side chains in the I-A^u p6 pocket compared to the corresponding positions of other class II MHC. The chemical environment of the p6 pocket is a combination of a hydrophobic neck and a moderately hydrophilic base (Figure 3B), which favors accommodation of a large, bulky residue in the bound peptide. There is a Gly66α in I-A^u where most other class II MHC have a large side chain that reduces the volume of the pocket. The shaft of the pocket is lined by hydrophobic residues Phe11β and Tyr30β and the aliphatic portions of Asn62α and Thr65α (Figure 3B). The base of the pocket is amphipathic with the capacity for both polar and nonpolar interactions.

A Key Interaction between MBP4 and the I-A^u p6 Pocket

In the structure, the p6 pocket is occupied by the MBP4 amino acid position (Figures 2 and 3B). Class II MHC-peptide complexes in normal registers occupy the p6 pocket with the P6 residue of the peptide. In the natural MBP sequence, residue number four is a lysine (Figure 4). In our structure, we have crystallized the MBP4-Lys $>$ MBP4-Tyr mutant of the MBP1-11 peptide due to its higher affinity for I-A^u (Figure 4) (Fairchild et al., 1993; Mason et al., 1995; Fugger et al., 1996). In the complex, the MBP4-Tyr side chain is deeply buried in the p6 pocket. The MBP4-Tyr aromatic ring is stacked between Phe11β and Tyr30β in the pocket's neck region, and the phenolic hydroxyl is H bonded to a water molecule linked to the base of the pocket (Figure 3B).

Why does Lys at the P4 position of native MBP destabilize the I-A^u complex relative to the MBP4-Tyr and MBP4-Ala variants? There are no charged MHC residues in this pocket to counterbalance the positive charge of the terminal Nϵ atom of a Lys, which likely accounts for the low affinity of the corresponding peptide/MHC interaction. However, stabilization forces are likely de-

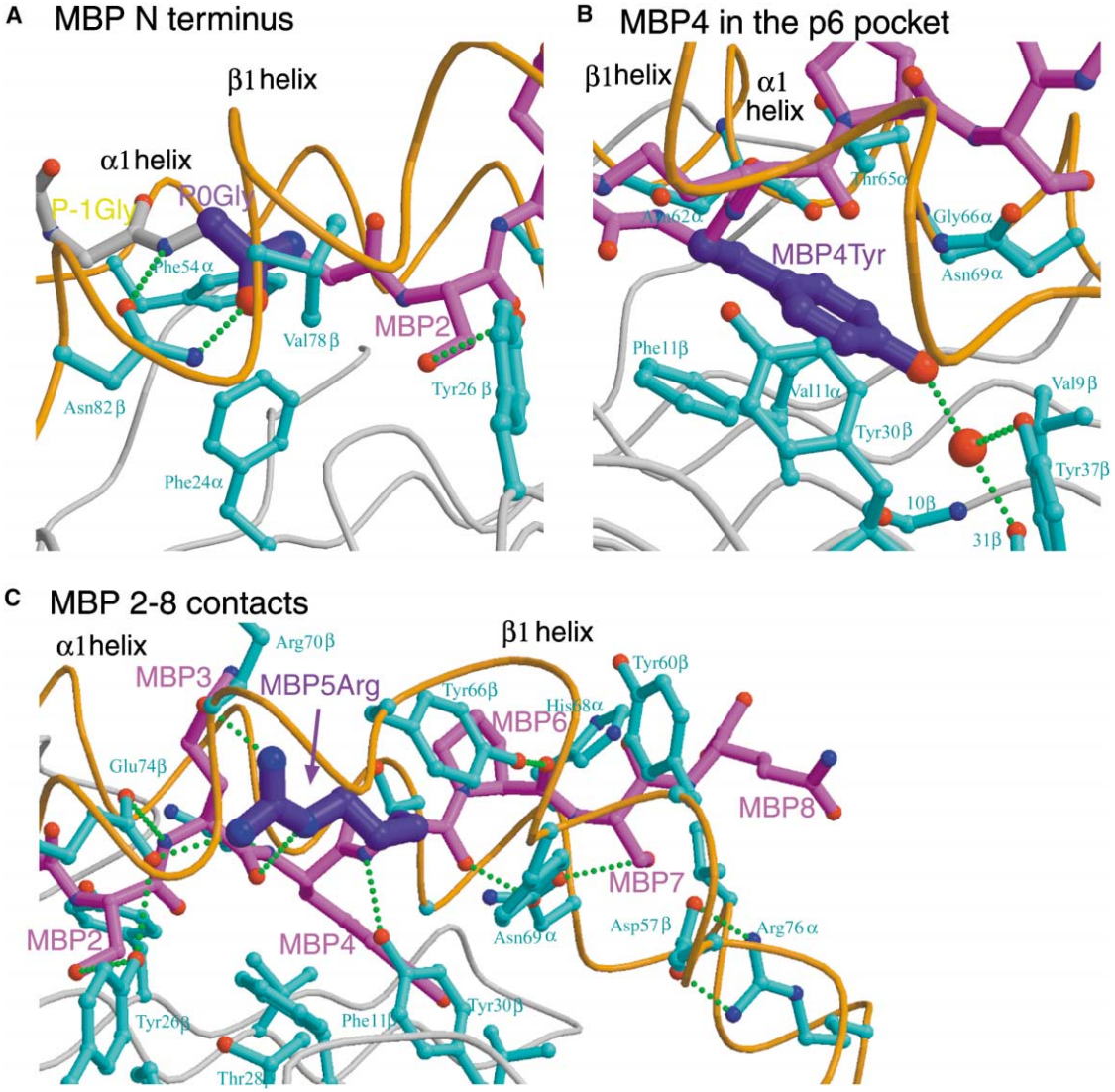

Figure 3. MBP Peptide Interactions with I-A^u

The orientation is as for the side view shown in Figure 1, with the peptide (purple) N terminus to the left and C terminus to the right. I-A^u β chain helix is in front (gray tube), and α chain helix is in back (gray) of the peptide. The residues of I-A^u which interact with the peptide are drawn as cyan. H bonds are indicated as green dots. Relevant residues are labeled for the (A) N-terminal, (B) central, and (C) more C-terminal MBP peptide interactions with I-A^u.

rived from: (1) the aliphatic portion of Lys making numerous van der Waals' interactions with the hydrophobic walls of the pocket, (2) the polarity of the Lys amino may coordinate water at the base of the pocket, as seen for P4-Tyr, and (3) flanking interactions between I-A^u and the MBP acetyl group, MBP2-Ser, MBP5-Arg, and MBP7-Ser. In total, the cumulative effect of these counterbalancing interactions appears sufficient to stabilize even the suboptimal MBP4-Lys ($t_{1/2} < 15$ min) sufficiently with I-A^u during T cell recognition for activation to occur (Fugger et al., 1996).

Structural Basis for the Functional Differences between Immunodominant MBP Peptide Variants

Substitution of MBP4-Lys with Ala, Val, or Tyr variants results in peptides that are ineffective, even antagonistic, in inducing EAE and have higher affinity for I-A^u (Figure 4). Further, the low affinity of the native (MBP4-Lys) I-A^u/MBP1-11 complex results in escape from negative selection of autoreactive T cells. The MBP4-Ala variant is more stable than MBP4-Lys but of lower stability than the MBP4-Tyr (Figure 4). The MBP4-Ala substitution would result in a loss of favorable hydrophobic interactions at the pocket neck, while removing the impact of an unfavorable positive charge. The progressive affinity increases as the size and hydrophobicity of MBP4 is increased (i.e., Ala, Val, Met, and Trp), and this can now simply be interpreted as an enhancement of the hydrophobic complementarity to the p6 pocket.

I-A^u is unusual in that MBP peptides as short as the N-terminal six residues of the Ac1-11 peptide bind to this MHC and can induce EAE (Gautam et al., 1992a, 1992b, 1994). Normal length peptides restricted by class II MHC molecules vary between ~12–17 amino acids.

A

	MHC class II pockets		p1	p2	p3	**p4**	p5	**p6**	p7	p8	**p9**	p10														
	MBP sequence				1	**2**	3	**4**	5	6	**7**	8	9	10	11	12	13	14	15	16	17	18				
Peptide No.	Length	Acetylation																								Binding capacity (IC50 nM)
1	11	Yes			A	S	Q	K	R	P	S	Q	R	H	G											>100μM
2	11	Yes			A	S	Q	**A**	R	P	S	Q	R	H	G											2500
3	11	Yes			A	S	Q	**Y**	R	P	S	Q	R	H	G											70
4	6	Yes			A	S	Q	K	R	P																>100μM
5	7	Yes			A	S	Q	K	R	P	S															>100μM
6	8	Yes			A	S	Q	K	R	P	S	Q														>100μM
7	9	Yes			A	S	Q	K	R	P	S	Q	R													>100μM
Pseudo-register:													p1	p2	p3	**p4**	p5	**p6**	p7	p8	**p9**	p10				
8	11	Yes			A	S	Q	K	R	P	S	Q	R	H	G											>100μM
9	12	Yes			A	S	Q	K	R	P	S	Q	R	H	G	S										>100μM
10	13	Yes			A	S	Q	K	R	P	S	Q	R	H	G	S	K									>100μM
11	14	Yes			A	S	Q	K	R	P	S	Q	R	H	G	S	K	Y								25000
12	15	Yes			A	S	Q	K	R	P	S	Q	R	H	G	S	K	Y	L							13333
13	16	Yes			A	S	Q	K	R	P	S	Q	R	H	G	S	K	Y	L	A						18182
14	16	Yes			A	S	Q	K	R	P	S	Q	R	S	K	Y	L	A	S	A						118
15	17	Yes			A	S	Q	K	R	P	S	Q	R	H	G	S	K	Y	L	A	T					3125
16	18	Yes			A	S	Q	K	R	P	S	Q	R	H	G	S	K	Y	L	A	T	A				270
17	20	Yes			A	S	Q	K	R	P	S	Q	R	H	G	S	K	Y	L	A	T	A	S	T		87
18	22	Yes			A	S	Q	K	R	P	S	Q	R	S	H	G	K	Y	L	A	T	A	S	T	M	D	15
19	9				A	S	Q	**Y**	R	P	S	Q	R														118
20	10			G	A	S	Q	K	R	P	S	Q	R														>100μM
21	10			G	A	S	Q	**Y**	R	P	S	Q	R														8.3
22	10			M	A	S	Q	K	R	P	S	Q	R														>100μM
23	10			M	A	S	Q	**Y**	R	P	S	Q	R														5.0
24	11		V	M	A	S	Q	K	R	P	S	Q	R														7143
25	12		D	V	M	A	S	Q	K	R	P	S	Q	R													4082
26	13		L	D	V	M	A	S	Q	K	R	P	S	Q	R												513
27	13		L	D	V	M	A	S	Q	**Y**	R	P	S	Q	R												11
Other known IAu binding peptides:																										
													R	H	G	S	K	Y	L	A	T	A	S	T		20
																S	K	Y	L	A	T	A	S	T	M	D 80
MBP-ala3		Yes			A	**A**	Q	**Y**	R	P	**A**	A	A	A	A											80
MBP-ala4		Yes			A	**A**	Q	**Y**	R	P	**A**	A														60
					A	**A**	Q	**Y**	R	P	**A**															60
					A	**A**	Q	**Y**	R	P																>100μM
				A	A	**A**	A	**Y**	R	A	**A**	A	A	A	A											31
Herpes VS		Yes			A	**A**	Q	**R**	R	P	S	R	P	F	R											>100μM
MBP 125-135			G	G	R	A	S	D	Y	K	S	A	H													
MBP 136-146			K	G	F	K	G	A	Y	D	A	Q	G													

B

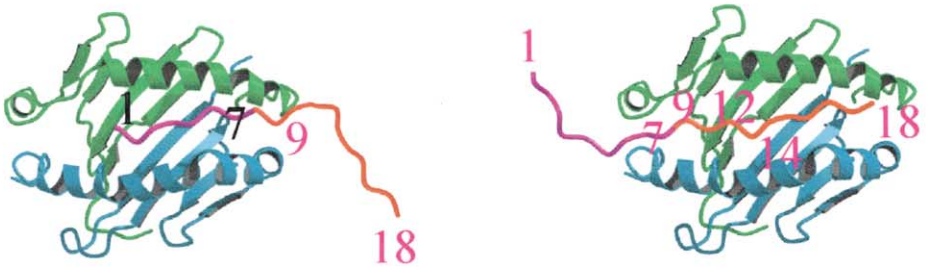

Figure 4. MBP Variants and the Presence of a Pseudo-Register in the MBP Sequence

The natural Ac1-11 sequence is peptide number 1, and the MBP sequence in our structure is peptide number 21. The experimental results shown in (A) are depicted in (B) as schematic models for the two possible registers of MBP1-7 (purple) and 8-18 (red) found, for example, in peptide number 16 from (A). The left model is the register seen in our structure (left), and the right model is the likely register adopted when MBP is extended at the C terminus, as shown for peptide numbers 8 through 18 in (A). The regions of the MBP peptide that are shown to extend out of the groove are arbitrarily drawn main chain atoms for illustrative purposes only. MBP125-136 and 136-146 (bottom two rows of [A]) have been predicted to bind in a canonical register (Loftus et al., 1999).

It is clear from this structure that MBP1-7 is located in the middle and C-terminal part of the peptide binding groove, with the MBP8-11 largely extended beyond the groove and playing no role in the interaction with I-A^u.

Inter- and Intramolecular Interactions by P5-Arg

Substitution of the MBP5-Arg affects both MHC and T cell recognition (Gautam et al., 1994; Wraith et al., 1992). Consistent with this data, in the structure the MBP5-Arg assumes integral structural roles in MHC stability and also influences the topology of the T cell epitope, through both *inter*molecular interactions with I-A^u and *intra*molecular interactions within the peptide (Figure 3C). The MBP5-Arg is located within a narrow and hydrophobic p7 pocket, in which the aliphatic portion of the MBP5-Arg is packed against the hydrophobic wall of the groove, and its guanidinium group is involved in an extensive hydrogen-bonding network (Figure 3C). The

MBP5-Arg guanidinium group is salt bridged to Glu74β of I-A^u in an intermolecular contact. Additionally, the MBP5-Arg Nη2 is H bonded to the MBP3-Gln Oε1 atom, and the MBP5-Arg Nε atom is H bonded to the peptide main chain (MBP3-Gln carbonyl oxygen) in intramolecular contacts (Figure 3C). These interactions effectively prevent clear solvent exposure of MBP5-Arg. The combination of both inter- and intramolecular contacts would be manifested in the mutational effects of MBP5-Arg (Gautam et al., 1994; Wraith et al., 1992) perturbing the MBP3-Gln position (a TCR contact), as well as the peptide-helix interaction that is constrained by the salt-bridge with Glu74β (Figures 1E and 3C).

The p9 Pocket

The p9 pocket of I-A^u is only partially filled by MBP7-Ser (Figures 2 and 3). This loose fit is compensated for, in part, by a hydrogen bond between MBP7-Ser Oγ and Oδ1 of Asn69β (Figure 3C). This hydrogen bond is, in fact, important to the overall I-A^u/MBP stabilization since deletion of MBP7-Ser severely reduces the I-A^u affinity for MBP1-6, but substitution to Thr maintains the interaction (Figure 4). The p9 pocket appears quite permissive to a variety of small residues. Beyond the p9 pocket, only the main chain of MBP8-Gln is visible in the electron density, with the remaining four MBP residues and the eight-residue linker to the β chain N terminus disordered.

Peptide Binding Specificity and a Cryptic Epitope

In the light of this structure, we asked what effect on binding is seen by extending the MBP peptide at the C terminus stepwise with the natural MBP sequence (Figure 4), as would be seen in vivo for naturally processed 12- to 18-mers presented by class II. We sequentially added one amino acid at a time to the C terminus of Ac1-11 to a final peptide length of 22 amino acids and expressed binding strength in terms of an inhibitory constant (IC_{50}) relative to a known tight binding peptide. As Figure 4 shows, these C-terminal additions resulted in a sequential increase in affinity from unmeasurably weak (peptide numbers four though ten, including Ac1-7[P4-Lys]) to 17 nM IC_{50} for peptide number 18 (Figure 4). We examined the sequences of the C-terminal additions and found that the major I-A^u contact positions MBP2, MBP4, and MBP9 are repeated at residues MBP12-Ser, MBP14-Tyr, and MBP17-Thr (instead of Ser) of MBP (Figure 4A). In fact, the MBP4-Lys, which is known to result in weak binding to I-A^u, is replaced by a Tyr in the C-terminal sequence, which causes a dramatic affinity increase. The three pseudo-motif residues apparent in the MHC contact residues of 1-7, have been enhanced in the C-terminal peptide by the substitution of the Tyr, as well as the completion of a more canonical length peptide that has the capacity to fill the entire peptide binding groove in a normal register, with all pockets occupied (Figure 4B) (Fairchild et al., 1993; Fugger et al., 1996). These features probably combine to render the C-terminal ten residues superior in binding affinity relative to the 1-7 sequence and therefore displace Ac1-7 from within the groove (model at the bottom of Figure 4). In general, class II peptides are 12–15 amino acids in length, so the higher affinity, longer epitope would better fit a canonical class II epitope than the MBP1-7, 1-9, or 1-11 peptides. Currently, there are no experimental data which demonstrate that the longer epitopes we produced synthetically can be generated in vivo by MBP processing (Fairchild et al., 1996). However, MBP5-20 can be generated from MBP1-20. Certainly a myriad of possibilities exist for naturally processed epitopes containing the higher affinity sequence(s).

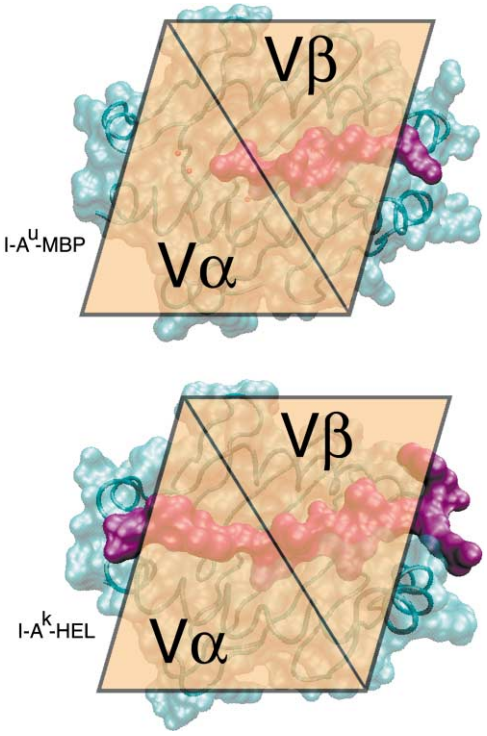

Figure 5. Schematic of Predicted TCR Footprints over the Composite Peptide-MHC Surfaces of I-A^u/MBP (top) and I-A^k-HEL (bottom)

To depict the natural Ac1-11 peptide, we have removed the residual leader peptide residues seen in our engineered construct (i.e., Figure 1B). An approximate diagonal orientation was achieved to represent the TCR Vα and Vβ chain overlying footprints on the MHC. The exact footprints cannot be known in the absence of a TCR/pMHC complex structure, so the orientations are ambiguous to allow for the range of orientations so far seen in class I and class II TCR/pMHC complex structures. In this representation, it is clear that the TCR Vα domain would be positioned largely over an empty region of the I-A^u groove in the MBP complex, irrespective of whether the exact orientation tends toward the perpendicular or diagonal.

Discussion

Our principal aim in this study was to provide molecular insight into the longstanding biochemical questions posed by the weakly binding, immunodominant epitope of MBP. The short-lived binding of the natural Ac1-11 MBP peptide in an unusual register, in a structurally indiscriminate I-A^u groove, leaves approximately one-third of the composite MHC-peptide binding groove unoccupied. The MBP4-Lys is constrained to occupy an incompatible, but energetically dominant, p6 pocket by noncanonical flanking interactions between what would normally be TCR contact residues and I-A^u. These flank-

ing interactions stabilize the suboptimal register sufficiently for recognition of MBP1-6 by encephalitogenic T cells (Gautam et al., 1994). However, the extremely short half-life of the complex formed by the binding of the N-terminal epitope of MBP to I-A^u results in the escape of autoreactive thymocytes from negative selection (Liu et al., 1995).

This structure further reveals a molecular explanation for the dramatic affinity increases resulting from extension of the C terminus of the MBP peptide. We find that a high affinity cryptic motif exists in this sequence that could bind I-A^u in a conventional register with enhanced MHC anchors (Figure 4). The potential of this flanking motif to mask the presentation of the encephalitogenic MBP1-9 peptide merits consideration as a form of immune subversion, as previously hypothesized by Sercarz and others (Sercarz et al., 1993; Fairchild et al., 1996). However, the naturally processed forms of MBP that might be involved in this register shifting are not known and if they exist would presumably be difficult to identify due to the induction of negative selection by high affinity, shifted MBP epitopes. Indeed, high affinity, immunogenic epitopes of this region of MBP have been characterized, but these epitopes are cryptic and cannot be generated by in vivo MBP processing (Fairchild et al., 1996).

The broader implications of this structure are that peptides binding in noncanonical and/or frame-shifted registers, which has been previously suggested as a possibility (Sercarz et al., 1993; Fairchild et al., 1996; Lee et al., 1998; McFarland et al., 1999), can, in fact, occur. It would appear that I-A MHC, which are frequently the restricting elements associated with autoimmunity, would be particularly prone to peptide frame-shifting due to their relatively promiscuous grooves that lead to extensive crossreactivity with peptides (Fremont et al., 1998; Scott et al., 1998). Register-shifting adds an additional dimension to the concept of T cell cross-reactivity, in that TCRs are clearly capable of recognizing noncanonical and shifted registers that would not be predicted using conventional TCR epitope alignments (McFarland et al., 1999; Garcia et al., 2001). The implications for autoimmunity are that many noncanonical and/or frame-shifted peptide registers are energetically unfavorable due to burial of N- or C-terminal charges in the groove and incompatible pockets. As such, these registers make transient complexes that may, like MBP, be poor inducers of negative selection of autoreactive T cells.

T Cell Epitope

The vast majority of T cells directed against the Ac1-11 epitope are sensitive to substitution of MBP residues MBP3-Gln, MBP5-Arg, and MBP6-Pro (Anderton et al., 1998; Wraith et al., 1989). From our structure, it is clear that these are the three most solvent exposed residues and would, therefore, be the preferred TCR contacts. In some T cell clones, such as 1934.4, there is some flexibility in the allowed substitutions at MBP3, but a strict requirement for the MBP6-Pro is maintained (Anderton et al., 1998). For the more crossreactive 172.10 T cells, multiple substitutions are allowed at MBP6 with less tolerance for MBP3 alterations (Anderton et al., 1998).

With the I-A^u/MBP1-11 structure, we can now examine data bearing on molecular mimicry of self-proteins by microbial pathogens, which has been suggested to be an environmental trigger for the development of autoimmune diseases (Oldstone, 1987; Wucherpfennig and Strominger, 1995). In one study, when the T cell epitope of the MBP Ac1-11 sequence was examined for potential microbial mimics, 832 candidate sequences were identified, of which 61 activated MBP-specific T cells (Grogan et al., 1999). All of these peptides contained Arg-Pro at P5-P6, and most contained a hydrophobic residue at P4. From consideration of both our structure and these sequence identities at key peptide positions, it is clear that these microbial mimic antigens would assume a similar noncanonical binding mode as MBP1-11. Hence, there appears to be a straightforward structural explanation for the activating potential of such peptides identified in vitro.

This structure also provides insight into the strong Vβ chain bias seen in MBP-specific TCRs (Acha-Orbea et al., 1988; Urban et al., 1988; Zamvil and Steinman, 1990). It is known from class I and class II TCR/MHC-peptide complex structures that the TCR Vα lies primarily over the peptide N-terminal region, and the Vβ lies over the C-terminal region (Figure 5) (Garcia et al., 1999; Hennecke and Wiley, 2001; Rudolph and Wilson, 2002). Therefore, the Vβ chain bias is likely explained by the majority of the MBP peptide epitope residing within the C-terminal region of the I-A^u groove, underneath the presumed TCR Vβ footprint. The available crystal structure coordinates for two TCR Vβ8.2 chains in complex with a class I MHC (2C TCR/H-2K^b-dEV8) and class II MHC (D10 TCR/I-A^k-CA) (Garcia et al., 1996, 1998; Reinherz et al., 1999) allow us to speculate on TCR(Vβ8.2)/I-A^u-Ac1-11 interactions. The two complexes span the range of orientation angles seen in TCR-MHC complexes, from the more diagonal seen in 2C/K^b to the less diagonal seen in D10/I-A^k. A constraint in this analysis is that the Vβ8 chain bias is antigen specific, so that there is almost certainly direct contact between the TCR CDR1β and/or CDR2β and the MBP peptide. In the D10/I-A^k complex, there is no CDR1β or CDR2β contact with peptide, indicating that this orientation is unlikely for MBP-specific TCRs (Reinherz et al., 1999). Rather, in the 2C/H-2K^b complex, CDR1β and CDR2β are oriented more over the C-terminal region of the groove, in close proximity to the peptide (Garcia et al., 1998). The region of the peptide that CDR1β and CDR2β will likely overlay in the complex, by extension from the four known TCR-pMHC complexes (Rudolph and Wilson, 2002), is centered at the P6-Pro in the I-A^u/MBP1-11 complex. Together, this cluster of amino acids presents a nonpolar patch to a TCR. One possible scenario for recognition of I-A^u/MBP1-11 is that the TCR orientation is rotated so that the conserved Vβ8 Tyr50β could form a contact with this nonpolar patch. Further structural studies will be required to gain further insight into the molecular details of TCR recognition (Thatte et al., 1999) of this unusual peptide-MHC complex.

Experimental Procedures

Protein Expression and Purification

The coding sequences for the extracellular domains of I-A^u α and β chains were amplified by PCR and subcloned into the pRMHa3

expression vector for expression in *Drosophila melanogaster* (Scott et al., 1996). The MBP1-11 sequence, with an additional N-terminal Gly residue to mimic the acetylation, was linked to the β chain N terminus through an eight residue GlySer linker. The C termini of each chain were cloned in frame with a Rhinovirus-C protease site that was linked to acidic or basic leucine zippers, followed by hexahistidine tags. Methodology for expression of class II MHC from *Drosophila melanogaster* is as previously described (Scott et al., 1996). The zippered MHC was cleaved with Rhino-C protease and digested with carboxypeptidase-A (1:100) prior to purification by mono-Q and superdex-200 gel filtration FPLC (Pharmacia, NJ). As a final step, the proteins were concentrated by centricon (Millipore) to ~15mg/ml in HBS, sterile-filtered, and stored at 4°C.

Expression and functional characterization of an I-A^u/MBP1-11 complex from baculovirus, using a honey bee mellitin secretion signal, has been previously described (Radu et al., 1998).

T Cell Activation Assays

172.10 hybridoma cells (Urban et al., 1988; a generous gift of Dr. Joan Goverman) were used in these assays. Hybridomas (5×10^4 cells/well) were incubated with plate-bound I-A^u/MBP1-11 complexes as described (Radu et al., 1998). Cells were stimulated for 24 hr and IL-2 levels in culture supernatants quantitated by IL-2 ELISA.

Crystallization, Data Collection, and Processing

The crystals of *Drosophila*-expressed I-A^u were grown from 20% MPEG-5K and 50 mM ammonium sulfide (pH 4.5) in the sitting drop format and were cryo-cooled for X-ray data collection in the presence of 20% glycerol. Complete data were collected from one crystal at beamline 7-1 at the Stanford Synchrotron Radiation Laboratory (SLAC, Stanford, CA) using 1.08 Å wavelength X-rays and image plates. The crystal diffracted to 2.2 Å resolution. A total of 120° oscillation images were collected under cryogenic conditions (T = 100 K). The data were indexed, integrated, and scaled with MOSFLM and SCALA (Kabsch, 1988), as integrated into the CCP4 program package (CCP4, 1994) in the orthorhombic spacegroup $C222_1$ with unit cell dimensions a = 99.15 Å, b = 110.59 Å, and c = 94.84 Å (Table 1).

Structure Determination and Refinement

The structure of I-A^u/MBP1-11 was determined with molecular replacement using the MOLREP program as implemented in the CCP4 package (CCP4, 1994). The I-A^k/HEL crystal structure (PDB ID: 1IAK) was used as a search model (Fremont et al., 1998). A rigid body refinement in CNS (Brünger et al., 1998) with data between 10–4 Å, treating the α1, β1, and α2 + β2 domains as three separate units, gave an initial model with an R factor of 0.442 for data in the 50–2.2 Å resolution range. The complex was then manually rebuilt using the program O (Jones et al., 1991) and then subjected to simulated annealing using the CNS torsion angle dynamics protocol and monitoring of R_{free} (Brünger, 1992). Extensive use of SIGMAA-weighted 2Fo-Fc and Fo-Fc omit maps was made to reduce the model bias (Read, 1986). Water molecules were automatically included with CNS and manually edited with electron density maps. Repeated iterations between manual rebuilding and minimization as well as B factor refinement finally resulted in a model with converged R factors of 24.8% and R_{free} of 27.8%. The stereochemistry of the model was analyzed with PROCHECK (Laskowski et al., 1993). A summary of the refinement statistics is given in Table 1.

Graphics

Figures were produced with Molscript, Raster3d, and Grasp (Kraulis, 1991; Merritt and Bacon, 1997; Nichols et al., 1991).

Affinity Purification of I-A^u Molecules

For binding studies, I-A^u molecules were purified from mouse B cell lymphoma 91.7 lysates using affinity chromatography. 91.7 cells were lysed for 30 min at 4°C with a lysis buffer of 50 mM Tris-HCL (pH 8.5), 1% NP40 (Fluka Biochemika, Buchs, Switzerland), 150 mM NaCl, and 2mM PMSF (CalBioChem, La Jolla, CA). I-A^u molecules were then purified using the anti-I-$A^{b,s,u}$ monoclonal antibody Y3JP coupled to Sepharose CL-4B beads (Janeway et al., 1984). I-A^u molecules were eluted with 50 mM diethylamine in 0.15 M NaCl containing 0.4% n-octylglucoside (pH 11.5). A 1/25 volume of 2.0 M Tris (pH 6.8) was added to the eluate to reduce the pH to ~8.0. The eluate was concentrated by centrifugation in Centriprep 30 concentrators at 2000 rpm (Amicon, Beverly, MA).

I-A^u Peptide Binding Assays

Quantitative peptide-I-A^u binding assays were based on the inhibition of binding of radiolabeled ROIV peptide (sequence YAHAAHAA HAAHAAHAA, IC50 of ROIV was 20 nM [Sette et al., 1990]). Assays were performed by coincubating purified I-A^u molecules (5 to 500 nM) for 48 hr with various concentrations (120 μM to 120 nM) of unlabeled peptide inhibitors and 1–10 nM ^{125}I-radiolabeled ROIV. The reaction was done at pH 7.0 in PBS containing 0.7% digitonin. For all assays, ROIV peptide was radiolabeled using the chloramine-T method (Sidney et al., 1998) and purified by size exclusion gel filtration HPLC (TosoHaas 16215, Montgomeryville, PA).

In preliminary experiments, I-A^u preparations were titered in the presence of a fixed amount of radiolabeled ROIV to determine the concentration of I-A^u molecules necessary to bind 10%–20% of the total radioactivity. In competitive assays, the concentration of peptide yielding 50% inhibition of the binding or the radiolabeled peptide was calculated. Under the conditions utilized, where [labeled peptide] < [MHC] and IC50 > [MHC], the measured IC50 values are reasonable approximations of true K_D values. Peptides were tested in two to four completely independent experiments.

Acknowledgments

We thank H. McDevitt, L. Steinman, and M. Davis for comments on the manuscript, I. Wilson for discussion of unpublished results, J. Ho for technical assistance, and the staff of the Stanford Synchrotron Radiation Laboratory for beamline resources and support. We are grateful to Mei Han for carrying out functional assays with soluble pMHC complexes and Mihail Firan for assistance with expression vector construction. K.C.G. is funded by NIH RO1 AI48540, the Multiple Sclerosis Society, and the Rita Allen Foundation. X.H. is supported by the American Heart Association, the California Cancer Research Program, and a Stanford Dean's Fellowship. E.S.W. is funded by grants RO1 AI/NS 42949 (NIH), RG-2411 (NMSS), and the Yellow Rose Foundation. J.S. and A.S. acknowledge NIH-NIAID contract N01-AI-95362.

Received: March 28, 2002
Revised: June 7, 2002

References

Acha-Orbea, H., Mitchell, D.J., Timmermann, L., Wraith, D.C., Tausch, G.S., Waldor, M.K., Zamvil, S.S., McDevitt, H.O., and Steinman, L. (1988). Limited heterogeneity of T cell receptors from lymphocytes mediating autoimmune encephalomyelitis allows specific immune intervention. Cell *54*, 263–273.

Anderton, S.M., Manickasingham, S.P., Burkhart, C., Luckcuck, T.A., Holland, S.J., Lamont, A.G., and Wraith, D.C. (1998). Fine specificity of the myelin-reactive T cell repertoire: implications for TCR antagonism in autoimmunity. J. Immunol. *161*, 3357–3364.

Anderton, S.M., Radu, C.G., Lowrey, P.A., Ward, E.S., and Wraith, D.C. (2001). Negative selection during the peripheral immune response to antigen. J. Exp. Med. *193*, 1–11.

Bouvier, M., and Wiley, D.C. (1998). Structural characterization of a soluble and partially folded class I major histocompatibility heavy chain/β_2m heterodimer. Nat. Struct. Biol. *5*, 377–384.

Brünger, A.T. (1992). Free R-value: a novel statistical quantity for assessing the accuracy of crystal structures. Nature *355*, 472–475.

Brünger, A.T., Adams, P.D., Clore, G.M., DeLano, W.L., Gros, P., Grosse-Kunstleve, R.W., Jiang, J.S., Kuszewski, J., Nilges, M., Pannu, N.S., et al. (1998). Crystallography and NMR system: a new software suite for macromolecular structure determination. Acta Crystallogr. D *54*, 905–921.

CCP4 (Collaborative Computational Project 4) (1994). The CCP4

suite: programs for protein crystallography. Acta Crystallogr. D *50*, 760–763.

Corper, A.L., Stratmann, T., Apostolopoulos, V., Scott, C.A., Garcia, K.C., Kang, A.S., Wilson, I.A., and Teyton, L. (2000). A structural framework for deciphering the link between I-Ag7 and autoimmune diabetes. Science *288*, 505–511.

Fairchild, P.J., Wildgoose, R., Atherton, E., Webb, S., and Wraith, D.C. (1993). An autoantigenic T cell epitope forms unstable complexes with class II MHC: a novel route for escape from tolerance induction. Int. Immunol. *5*, 1151–1158.

Fairchild, P.J., Pope, H., and Wraith, D.C. (1996). The nature of cryptic epitopes within the self-antigen myelin basic protein. Int. Immunol. *8*, 1035–1043.

Fremont, D.H., Monnaie, D., Nelson, C.A., Hendrickson, W.A., and Unanue, E.R. (1998). Crystal structure of I-Ak in complex with a dominant epitope of lysozyme. Immunity *8*, 305–317.

Fugger, L., Liang, J., Gautam, A., Rothbard, J.B., and McDevitt, H.O. (1996). Quantitative analysis of peptides from myelin basic protein binding to the MHC class II protein, I-A^u, which confers susceptibility to experimental allergic encephalomyelitis. Mol. Med. *2*, 181–188.

Garcia, K.C., Degano, M., Stanfield, R.L., Brunmark, A., Jackson, M.R., Peterson, P.A., Teyton, L., and Wilson, I.A. (1996). An alphabeta T cell receptor structure at 2.5 Å and its orientation in the TCR-MHC complex. Science *274*, 209–219.

Garcia, K.C., Degano, M., Pease, L.R., Huang, M., Peterson, P.A., Teyton, L., and Wilson, I.A. (1998). Structural basis of plasticity in T cell receptor recognition of a self peptide-MHC antigen. Science *279*, 1166–1172.

Garcia, K.C., Teyton, L., and Wilson, I.A. (1999). Structural basis of T cell recognition. Annu. Rev. Immunol. *17*, 369–397.

Garcia, K.C., Radu, C.G., Ho, J., Ober, R.J., and Ward, E.S. (2001). Kinetics and thermodynamics of T cell receptor- autoantigen interactions in murine experimental autoimmune encephalomyelitis. Proc. Natl. Acad. Sci. USA *98*, 6818–6823.

Gautam, A.M., Pearson, C.I., Sinha, A.A., Smilek, D.E., Steinman, L., and McDevitt, H.O. (1992a). Inhibition of experimental autoimmune encephalomyelitis by a nonimmunogenic non-self peptide that binds to I-Au. J. Immunol. *148*, 3049–3054.

Gautam, A.M., Pearson, C.I., Smilek, D.E., Steinman, L., and McDevitt, H.O. (1992b). A polyalanine peptide with only five native myelin basic protein residues induces autoimmune encephalomyelitis. J. Exp. Med. *176*, 605–609.

Gautam, A.M., Lock, C.B., Smilek, D.E., Pearson, C.I., Steinman, L., and McDevitt, H.O. (1994). Minimum structural requirements for peptide presentation by major histocompatibility complex class II molecules: implications in induction of autoimmunity. Proc. Natl. Acad. Sci. USA *91*, 767–771.

Goverman, J. (1999). Tolerance and autoimmunity in TCR transgenic mice specific for myelin basic protein. Immunol. Rev. *169*, 147–159.

Grogan, J.L., Kramer, A., Nogai, A., Dong, L., Ohde, M., Schneider-Mergener, J., and Kamradt, T. (1999). Cross-reactivity of myelin basic protein-specific T cells with multiple microbial peptides: experimental autoimmune encephalomyelitis induction in TCR transgenic mice. J. Immunol. *163*, 3764–3770.

Harrington, C.J., Paez, A., Hunkapiller, T., Mannikko, V., Brabb, T., Ahearn, M., Beeson, C., and Goverman, J. (1998). Differential tolerance is induced in T cells recognizing distinct epitopes of myelin basic protein. Immunity *8*, 571–580.

Hennecke, J., and Wiley, D.C. (2001). T cell receptor-MHC interactions up close. Cell *104*, 1–4.

Janeway, C.A., Jr., Conrad, P.J., Lerner, E.A., Babich, J., Wettstein, P., and Murphy, D.B. (1984). Monoclonal antibodies specific for Ia glycoproteins raised by immunization with activated T cells: possible role of T cell bound Ia antigens as targets of immunoregulatory T cells. J. Immunol. *132*, 662–667.

Jones, T.A., Zou, J.Y., Cowan, S.W., and Kjeldgaard, M. (1991). Improved methods for binding protein models in electron density maps and the location of errors in these models. Acta Crystallogr. D *47*, 110–119.

Kabsch, W. (1988). Evaluation of single crystal x-ray diffraction data from a position sensitive detector. J. Appl. Crystallogr. *21*, 916–924.

Kraulis, P.J. (1991). MOLSCRIPT. J. Appl. Crystallogr. *24*, 946–950.

Laskowski, R.A., MacArthur, M.W., Moss, D.S., and Thornton, J.M. (1993). PROCHECK: a program to check the stereochemical quality of protein structures. J. Appl. Crystallogr. *26*, 283–291.

Latek, R.R., Suri, A., Petzold, S.J., Nelson, C.A., Kanagawa, O., Unanue, E.R., and Fremont, D.H. (2000). Structural basis of peptide binding and presentation by the type I diabetes-associated MHC class II molecule of NOD mice. Immunity *12*, 699–710.

Lee, C., Liang, M.N., Tate, K.M., Rabinowitz, J.D., Beeson, C., Jones, P.P., and McConnell, H.M. (1998). Evidence that the autoimmune antigen myelin basic protein (MBP) Ac1-9 binds towards one end of the major histocompatibility complex (MHC) cleft. J. Exp. Med. *187*, 1505–1516.

Lee, K.H., Wucherpfennig, K.W., and Wiley, D.C. (2001). Structure of a human insulin peptide-HLA-DQ8 complex and susceptibility to type 1 diabetes. Nat. Immunol. *2*, 501–507.

Liu, G.Y., Fairchild, P.J., Smith, R.M., Prowle, J.R., Kioussis, D., and Wraith, D.C. (1995). Low avidity recognition of self-antigen by T cells permits escape from central tolerance. Immunity *3*, 407–415.

Loftus, C., Huseby, E., Gopaul, P., Beeson, C., and Goverman, J. (1999). Highly cross-reactive T cell responses to myelin basic protein epitopes reveal a nonpredictable form of TCR degeneracy. J. Immunol. *162*, 6451–6457.

Madden, D.R. (1995). The three-dimensional structure of peptide-MHC complexes. Annu. Rev. Immunol. *13*, 587–622.

Mason, K., Denney, D.W., Jr., and McConnell, H.M. (1995). Kinetics of the reaction of a myelin basic protein peptide with soluble IAu. Biochemistry *34*, 14874–14878.

McFarland, B.J., Sant, A.J., Lybrand, T.P., and Beeson, C. (1999). Ovalbumin(323-339) peptide binds to the major histocompatibility complex class II I-A^d protein using two functionally distinct registers. Biochemistry *39*, 16663–16670.

Merritt, E.A., and Bacon, D.J. (1997). Raster3D photorealistic molecular graphics. Methods Enzymol. *277*, 505–524.

Nichols, A., Sharp, K.A., and Honig, B. (1991). Protein folding and association: insights from the interfacial and thermodynamic properties of hydrocarbons. Proteins *11*, 281–296.

Oldstone, M.B. (1987). Molecular mimicry and autoimmune disease. Cell *50*, 819–820.

Pearson, C.I., van Ewijk, W., and McDevitt, H.O. (1997). Induction of apoptosis and T helper 2 (Th2) responses correlates with peptide affinity for the major histocompatibility complex in self-reactive T cell receptor transgenic mice. J. Exp. Med. *185*, 583–599.

Pearson, C.I., Gautam, A.M., Rulifson, I.C., Liblau, R.S., and McDevitt, H.O. (1999). A small number of residues in the class II molecule I-Au confer the ability to bind the myelin basic protein peptide Ac1-11. Proc. Natl. Acad. Sci. USA *96*, 197–202.

Radu, C.G., Ober, B.T., Colantonio, L., Qadri, A., and Ward, E.S. (1998). Expression and characterization of recombinant soluble peptide: I-A complexes associated with murine experimental autoimmune diseases. J. Immunol. *160*, 5915–5921.

Radu, C.G., Anderton, S.M., Firan, M., Wraith, D.C., and Ward, E.S. (2000). Detection of autoreactive T cells in H-2^u mice using peptide-MHC multimers. Int. Immunol. *11*, 1553–1560.

Rammensee, H.G., Friede, T., and Stevanoviic, S. (1995). MHC ligands and peptide motifs: first listing. Immunogenetics *41*, 178–228.

Read, R.J. (1986). SIGMAA. Acta Crystallogr. A *42*, 140–159.

Reinherz, E.L., Tan, K., Tang, L., Kern, P., Liu, J., Xiong, Y., Hussey, R.E., Smolyar, A., Hare, B., Zhang, R., et al. (1999). The crystal structure of a T cell receptor in complex with peptide and MHC class II. Science *286*, 1913–1921.

Rudolph, M.G., and Wilson, I.A. (2002). The specificity of TCR/pMHC interaction. Curr. Opin. Immunol. *14*, 52–65.

Scott, C.A., Garcia, K.C., Carbone, F.R., Wilson, I.A., and Teyton, L. (1996). Role of chain pairing for the production of functional soluble

IA major histocompatibility complex class II molecules. J. Exp. Med. *183*, 2087–2095.

Scott, C.A., Peterson, P.A., Teyton, L., and Wilson, I.A. (1998). Crystal structures of two I-Ad-peptide complexes reveal that high affinity can be achieved without large anchor residues. Immunity *8*, 319–329.

Sercarz, E.E., Lehmann, P.V., Ametani, A., Benichou, G., Miller, A., and Moudgil, K. (1993). Dominance and crypticity of T cell antigenic determinants. Annu. Rev. Immunol. *11*, 729–766.

Sette, A., Sidney, J., Albertson, M., Miles, C., Colon, S.M., Pedrazzini, T., Lamont, A.G., and Grey, H.M. (1990). A novel approach to the generation of high affinity class II-binding peptides. J. Immunol. *145*, 1809–1813.

Sidney, J., Southwood, S., Oseroff, C., del Guercio, M.F., Sette, A., and Grey, H. (1998). The measurement of MHC/peptide interactions by gel infiltration. Curr. Prot. Immunol. *18*, 3.1–3.19.

Smith, K.J., Pyrdol, J., Gauthier, L., Wiley, D.C., and Wucherpfennig, K.W. (1998). Crystal structure of HLA-DR2 (DRA*0101, DRB1*1501) complexed with a peptide from human myelin basic protein. J. Exp. Med. *188*, 1511–1520.

Steinman, L. (1996). Multiple sclerosis: a coordinated immunological attack against myelin in the central nervous system. Cell *85*, 299–302.

Stern, L.J., and Wiley, D.C. (1994). Antigenic peptide binding by class I and class II histocompatibility proteins. Structure *2*, 245–251.

Thatte, J., Qadri, A., Radu, C., and Ward, E.S. (1999). Molecular requirements for T cell recognition by a major histocompatibility complex class II-restricted T cell receptor: the involvement of the fourth hypervariable loop of the valpha domain. J. Exp. Med. *189*, 509–520.

Tisch, R., and McDevitt, H. (1996). Insulin-dependent diabetes mellitus. Cell *85*, 291–297.

Urban, J.L., Kumar, V., Kono, D.H., Gomez, C., Horvath, S.J., Clayton, J., Ando, D.G., Sercarz, E.E., and Hood, L. (1988). Restricted use of T cell receptor V genes in murine autoimmune encephalomyelitis raises possibilities for antibody therapy. Cell *54*, 577–592.

Wang, C.R., Castano, A.R., Peterson, P.A., Slaughter, C., Lindahl, K.F., and Deisenhofer, J. (1995). Nonclassical binding of formylated peptide in crystal structure of the MHC class Ib molecule H2–M3. Cell *82*, 655–664.

Wraith, D.C., Smilek, D.E., Mitchell, D.J., Steinman, L., and McDevitt, H.O. (1989). Antigen recognition in autoimmune encephalomyelitis and the potential for peptide-mediated immunotherapy. Cell *59*, 247–255.

Wraith, D.C., Bruun, B., and Fairchild, P.J. (1992). Cross-reactive antigen recognition by an encephalitogenic T cell receptor. Implications for T cell biology and autoimmunity. J. Immunol. *149*, 3765–3770.

Wucherpfennig, K.W., and Strominger, J.L. (1995). Molecular mimicry in T cell-mediated autoimmunity: viral peptides activate human T cell clones specific for myelin basic protein. Cell *80*, 695–705.

Zamvil, S.S., and Steinman, L. (1990). The T lymphocyte in experimental allergic encephalomyelitis. Annu. Rev. Immunol. *8*, 579–621.

Zamvil, S.S., Mitchell, D.J., Moore, A.C., Kitamura, K., Steinman, L., and Rothbard, J.B. (1986). T-cell epitope of the autoantigen myelin basic protein that induces encephalomyelitis. Nature *324*, 258–260.

Zarutskie, J.A., Sato, A.K., Rushe, M.M., Chan, I.C., Lomakin, A., Benedek, G.B., and Stern, L.J. (1999). A conformational change in the human major histocompatibility complex protein HLA-DR1 induced by peptide binding. Biochemistry *38*, 5878–5887.

Accession Numbers

The coordinates of I-A^u/MBP1-11 have been deposited in the RCSB PDB under accession code 1K2D.